Slow light excitation in tapered 1D photonic crystals: theory

D. Yudistira *, H.J.W.M. Hoekstra, M. Hammer and D.A.I. Marpaung.
Mesa+ Research institute, University of Twente,
P.O. Box 217, 7500 AE Enschede, The Netherlands
(*author for correspondence: E-mail: d.yudistira@el.utwente.nl)

Abstract. *Slow light (SL) states corresponding to wavelength regions near the bandgap edge of grated structures are known to show strong field enhancement. Such states may be excited efficiently by well-optimised adiabatic transitions in grated structures, e.g., by slowly turning on the modulation depth. To study adiabatic excitations, a detailed research in 1D is performed to obtain insight into the relation between the device parameters and properties like enhancement and modal reflection. The results enable the design of an adiabatic device for efficient excitation of SL states in 1D. The effect of small wavelength variations as well as small fluctuations in the modulation depth of the grating has been investigated.*

Key words: adiabatic excitation, coupled mode theory, photonic crystals, slow light

1. Introduction

Recently, periodic dielectric structures (i.e. photonic crystals (PCs)) have attracted much interest by a large number of researchers. The main reason for that is due to the fact that materials with a photonic band gap can be realised by means of a proper choice of both lattice structure and index contrast. This phenomenon leads to variety of (possible) applications such as the inhibition of spontaneous emission (Yablonovitch 1987), low loss waveguides with sharp bends (Mekis *et al.* 1996), narrow-band filters, and strong field enhancement related to low group velocity, i.e. slow light (SL), modes propagating at state near the band edge (Sakoda *et al.* 1996; Notomi *et al.* 2001; Povinelli *et al.* 2005). Due to the mismatch of both modal profiles and phase velocities between the incoming propagating wave the modes in SL devices (e.g. grating), direct excitation of SL mode will cause high losses (Notomi *et al.* 2001). One promising technique that has been introduced in several papers to overcome this problem is so-called adiabatic excitation (Povinelli *et al.* 2005; Johnson *et al.* 2002). By means of gradually changing index or geometry of the gratings, it is possible to change the profile of an incoming wave gradually into that of the SL mode. Thus, the effects of profile mismatch and so of losses can be minimised. Even tough a topic about gratings with slowly varying index or geometry is rather old and it has been subjected to research by many researches (Matuschek *et al.* 1997; Sipe *et al.* 1994; Spielmann *et al.* 1994). However, from the author's knowledge, there is no paper specifically covered an issue about the application such gratings for SL excitation.

In this paper, we will present a theory for SL excitation in 1D. In particular, we discuss the relation between device parameters, like modulation depth, and modal properties, like power enhancement and modal reflection. A structure for the adiabatic excitation of SL mode in 1D gratings is proposed. We also investigate the effect of small wavelength

variations as well as index fluctuations, on the excitation efficiency of SL modes in proposed adiabatic structure. The rest of the paper is organized as follows: In the Section 2, we will present theory of uniform 1D grating. The relation between modal and structural parameters is treated in Section 3. The study of adiabatic excitation is given in Section 4 and in Section 5 the effects of small wavelength and fluctuations are discussed. We end this paper with conclusion given in section 6.

2. Basic theory

In this section we will consider basic equations for optical fields propagating through uniform and modulated 1D grating, consisting of two different layers (index and thickness, n_q and d_q, respectively, $q=1,2$), in a direction perpendicular to the interfaces (see Fig. (1)). A time dependence $e^{i\omega t}$ is assumed but suppressed. In addition, a coupled mode (CM) model is introduced for the description of light in a 1D grating with a slowly varying modulation depth, n_m. The field equation to be solved is:

$$[\partial_{zz} + k_0^2 n^2(z)]E(z) = 0, \tag{1}$$

where k_0 is the wavenumber and *n* is the refractive index. The field solutions to Equation (1) in each layer *p* can be written as the sum of right and left running plane waves:

$$E = v + w;\ v \propto e^{-i\alpha_p z}, w \propto e^{i\alpha_p z},\ \alpha_p \equiv k_0 n_p,\ p = 1,2. \tag{2}$$

For a uniform grating it follows from the Floquet-Bloch theorem that there exist modes for which $E(z+\Lambda) = e^{-i\beta\Lambda}E(z)$, with Λ the grating period. If we consider a symmetric unit cell (with $-d_1/2 < z < \Lambda - d_1/2$, see Fig. (2)) it follows:

$$\begin{pmatrix} v \\ w \end{pmatrix}_{\Lambda - d_1/2} = M \begin{pmatrix} v \\ w \end{pmatrix}_{-d_1/2} = e^{-i\beta\Lambda} \begin{pmatrix} v \\ w \end{pmatrix}_{-d_1/2},\ M \equiv \begin{pmatrix} 1/t^* & r/t \\ r^*/t^* & 1/t \end{pmatrix}, \text{ with } |M| = 1. \tag{3}$$

Here *r* and *t* are the reflection and transmission coefficients for the considered unit cell, the asterisk (*) denotes the complex conjugate and we have used the general properties of the scattering matrix (Haus 1982), leading to $|r|^2 + |t|^2 = 1$ and $r^* t + t^* r = 0$. The eigenvalues of matrix *M* are:

$$\chi_\pm = R \pm \sqrt{R^2 - 1} (= e^{-i\beta_\pm \Lambda}), \tag{4}$$

with $R \equiv \frac{1}{2t} + \frac{1}{2t^*} = Re(t)/|t|^2$. We will consider (in most cases) only running waves corresponding to $R^2 \le 1$. The corresponding eigenvectors are:

$$\begin{pmatrix} 1 \\ \gamma_\pm \end{pmatrix},\ \gamma_\pm \equiv \frac{t}{r}\chi_\pm + \frac{1}{r^*}. \tag{5}$$

It can be shown from the above relations between *r* and *t* that $\gamma_+ \gamma_- = 1$, both $\gamma_\pm$ are real, and that $\gamma_\pm = \mathrm{Re}(1/r) = +1$ or -1 at the band edge (transition between running and evanescent modes, corresponding to $R^2 = 1$). We choose $|\gamma_+| \le |\gamma_-|$, so that for $R^2 \le 1$ the subscripts + (-) correspond to right (left) running modal waves.

The normalized eigenvectors at positions $z = m\Lambda - d_1/2$ are given by:

$$\begin{pmatrix} v \\ w \end{pmatrix}_{\pm,-d_1/2} = \frac{1}{\sqrt{\alpha_1(\pm 1 \mp |\gamma_\pm|^2)}} \begin{pmatrix} 1 \\ \gamma_\pm \end{pmatrix}, \tag{6}$$

whereby the following holds for the modal power:

$$P_\pm = \alpha_p(|v_\pm|^2 - |w_\pm|^2) = \pm 1. \tag{7}$$

The latter is defined by:

$$P_\pm = \alpha_p \begin{pmatrix} v_\pm^* & w_\pm^* \end{pmatrix} \begin{pmatrix} 1 & 0 \\ 0 & -1 \end{pmatrix} \begin{pmatrix} v_\pm \\ w_\pm \end{pmatrix}. \tag{8}$$

Note that (modal) cross product is zero, which follows from Equation (6) and the property $\gamma_+\gamma_- = 1$. The latter holds for all positions in all layers and the modal power is a conserved quantity in a uniform grating.

The modal propagation in layers of type *p* is given by:

$$\begin{pmatrix} v_\pm \\ w_\pm \end{pmatrix}_{z+\Delta z} = \begin{pmatrix} e^{-i\alpha_p \Delta z} & 0 \\ 0 & e^{i\alpha_p \Delta z} \end{pmatrix} \begin{pmatrix} v_\pm \\ w_\pm \end{pmatrix}_z. \tag{9}$$

The modal transfer from layer 1 to layer 2 (at $z = m\Lambda$) can be calculated to be given by:

$$\begin{pmatrix} v_\pm \\ w_\pm \end{pmatrix}_{p\Lambda^+} = T_{12} \begin{pmatrix} v_\pm \\ w_\pm \end{pmatrix}_{p\Lambda^-} ; \; T_{12} \equiv \frac{1}{2n_2} \begin{pmatrix} n_1 + n_2 & n_2 - n_1 \\ n_2 - n_1 & n_1 + n_2 \end{pmatrix}. \tag{10}$$

Here the superscript + (-) (in $p\Lambda^+$) indicates a *z* value just right (left) of the indicated interface. A similar expression as above holds for the modal transfer from layer 2 to 1. With Equations (8-10) it is easy to show that the power in a uniform grating is constant along *z*, as it should. The field in a grating can be expressed by:

$$E(z) = a(v_+ + w_+) + b(v_- + w_-), \tag{11}$$

with *a* and *b* constants, and the net power along *z* is given by $P = |a|^2 - |b|^2$.

As a measure for the power enhancement for a certain set of grating parameters we define:

$$\eta \equiv \frac{|v_+|^2 + |w_+|^2}{|v_+|^2 - |w_+|^2}, \tag{12}$$

being the ratio of the total power (sum of power of left and right going modes) and the net power of a certain mode. The quantity is position dependent (constant within each layer), but not in a critical way, as follows from numerical calculations. In this paper we will evaluate it at positions $z = m\Lambda - d_1/2$, leading to (see Equation (6)):

$$\eta = \frac{1+\gamma_+^2}{1-\gamma_+^2} = \left(\frac{\gamma_-^2 + 1}{\gamma_-^2 - 1} \right). \tag{13}$$

Numerical results indicate that $\eta \propto\sim 1/v_g$, with $v_g (\equiv \partial\omega/\partial\beta)$ the group velocity. In the below a 1D grating is considered with a slowly varying modulation dept, n_m, in the region $z \in [0, L]$. The modulation depth changes from unit cell to unit cell (see Fig. (1)). The total field is given by equation 11, but now modal amplitudes *a* and *b* (still constant within a unit cell) vary from unit cell to unit cell, and $v_\pm$ and $w_\pm$ correspond to the considered unit cell, with

$$\begin{pmatrix} v_{\pm} \\ w_{\pm} \end{pmatrix}_{p\Lambda^{+};n_{m,p+1}} = e^{\mp i\varphi_p} \begin{pmatrix} v_{\pm} \\ w_{\pm} \end{pmatrix}_{0\Lambda^{+};n_{m,p+1}}, \ \varphi_p = \Lambda \sum_{l=1}^{p} \beta_l . \tag{14}$$

Here, $n_{m,p}$ is the modulation depth in the p^{th} unit cell and we dropped the subscript + in β. Note that the fields $v_{\pm}$ and $w_{\pm}$ at other positions in the unit cell than $p\Lambda^{+}$ can be calculated with the transfer matrix method, similarly as in Equations (9) and (10).

At a step in the modulation depth the modal transmission is no longer unity, and modal reflection will occur. The scatter process may be described by:

$$\begin{pmatrix} a_{p+1} \\ b_p \end{pmatrix} = S \begin{pmatrix} b_{p+1} \\ a_p \end{pmatrix}, \ S \equiv \begin{pmatrix} r_r & t \\ t & r_l \end{pmatrix}, \tag{15}$$

with *S* the scattering matrix. Note that the above (matrix transfer) treatment is still exact, unlike the CM theory given below.

In a CM picture the behavior of light in the smoothly varying grating can be described by (Kogelnik *et al.* 1971) the following CM equations (CMEs):

$$\partial_z \begin{pmatrix} a \\ b \end{pmatrix} = -iK \begin{pmatrix} a \\ b \end{pmatrix}, \ K \equiv \begin{pmatrix} \kappa_{aa} & \kappa_{ab} \exp(-2i\int_0^z \beta dz') \\ -\kappa_{ba} \exp(2i\int_0^z \beta dz') & -\kappa_{bb} \end{pmatrix}, \tag{16}$$

where *a*, *b* and the coefficients κ vary slowly as a function of *z*. Form conservation of energy ($\partial_z(|a|^2 - |b|^2) = 0$) it can be derived that:

$$\kappa_{aa} = \kappa_{bb} \in \text{Re}, \ \kappa_{ab} = \kappa_{ba}^{*}, \tag{17}$$

whereby the first equality follows from symmetry considerations. Integration of Equation (16) over one unit cell leads to:

$$\begin{pmatrix} a \\ b \end{pmatrix}_{(p+1)\Lambda} = e^{-i\tilde{K}_p \Lambda} \begin{pmatrix} a \\ b \end{pmatrix}_{p\Lambda}; \tilde{K}_p \equiv \begin{pmatrix} \tilde{\kappa}_{aa} & \tilde{\kappa}_{ab} \\ -\tilde{\kappa}_{ba} & -\tilde{\kappa}_{bb} \end{pmatrix} = \frac{1}{\Lambda} \int_{p\Lambda}^{(p+1)\Lambda} K dz , \tag{18}$$

whereby relations equivalent to Equation (17) hold for the elements of $\tilde{K}_p$. These can be calculated for a certain parameter set, by comparing Equations (15) and (18). First, the elements of *S* have to be calculated. Considering an incoming field from the left (see Fig. (3)) at the interface at $z = p\Lambda$, with amplitude $a_p = 1$, it can be derived from the above that (see also Equation (10)):

$$T_{12}' \left[\begin{pmatrix} v_{+} \\ w_{+} \end{pmatrix} + r_l \begin{pmatrix} v_{-} \\ w_{-} \end{pmatrix} \right]_{p\Lambda^{-},n_{m,p}} = t \begin{pmatrix} v_{+} \\ w_{+} \end{pmatrix}_{p\Lambda^{+},n_{m,p+1}} . \tag{19}$$

Here the prime indicates that the two involved unit cells differ in modulation depth. From Equation (19) one can calculate the values of r_r, t and $r_l (= -r_r^{*} t / t^{*})$, where the latter equality follows from the general properties of the scattering matrix, *S*. The fields $v_{\pm}$ and $w_{\pm}$ can be calculated using Equations (5-6) including the phase term $\exp(\mp i\varphi_p)$ defined in Equation (14).

Next, rewriting Equation (15) as

$$\begin{pmatrix} a_{p+1} \\ b_{p+1} \end{pmatrix} = M_p \begin{pmatrix} a_p \\ b_p \end{pmatrix}, \ M_p \equiv \begin{pmatrix} 1/t^{*} & r_r / t \\ r_r^{*} / t^{*} & 1/t \end{pmatrix} \tag{20}$$

and comparing the result with Equation (18) it follows:

$$\tilde{K}_p = -i \ln M_p / \Lambda . \qquad (21)$$

From the properties of M_p (eigenvalues and eigenvectors of the form $\exp(\pm i\theta_p)$ and $(1 \quad d)^t$, $\left(d^* \quad 1\right)^t$, respectively) the relations Equation (17) can easily be derived.

The most relevant elements of matrix $\tilde{K}_p$ are the off-diagonal elements, which describe modal reflection at steps in the modulation depth. The diagonal terms only introduce a modal phase shift, which is relatively small as it appears from numerical calculations that $|\tilde{\kappa}_{aa}| \ll |\tilde{\kappa}_{ab}|$, and so $|\kappa_{aa}| \ll |\kappa_{ab}|$. For these reasons we will concentrate in the below mainly on the coupling parameter $\kappa (\equiv |\tilde{\kappa}_{ab}|)$.

3 Relations between modal and structural parameters

In this section, numerically calculated approximate relations, including their wavelength dependence, between modal parameters (power enhancement, η, and coupling parameter, κ) and structural parameters will be presented. For this purpose, a model structure is considered with the following parameters: layer thicknesses $d_1 = d_2 = 0.1613 \mu m$, indices $n_{1/2} = n_{av} +/- n_m$, with an average index of $n_{av} = 1.55$. The parameters correspond to a bandgap at $\lambda = 1 \mu m$ for $n_m \to 0$. The structural parameters to be varied are the modulation depth, n_m, and its rate of change at interfaces between two unit cells, Δn_m ($\approx \Lambda \partial_z n_m$, in a CM picture, where variations are assumed to be smooth).

We have studied the above relations for a not too large modulations depth, $0 < n_m \leq 0.3$, and a wavelength region corresponding to $0 < n_{m,edge} \leq 0.3$, where $n_{m,edge}$ depends linearly on the wavelength (see Fig. (4)). Here $n_{m,edge}$ is defined as the modulation depth corresponding to the band-edge for a given wavelength. In the below we will use the parameter $n_{m,edge}$ to indicate the wavelength in order to obtain more transparent expressions.

Careful fitting of numerical results in the region $0 < n_m \leq 0.3$, at wavelengths for which $n_m < n_{m,edge}$, leads to the following results:

$$\kappa \approx C n_{m,edge} \partial_z n_m / h, \;\; h \equiv n_{m,edge}^2 - n_m^2, \; C = 0.52, \qquad (22)$$

and

$$\eta \approx n_{m,edge} / \sqrt{h} . \qquad (23)$$

Figures (5a) and (5b) show a few graphs illustrating Equations (22) and (23), respectively.

4. Adiabatic excitation

In adiabatically varying structures (see Fig. (6)) the changes are that slow that only little mode conversion takes place. Form CM theory it can be shown that two modes show little interaction if the ratio of phase-mismatch and coupling constant is small. As a tapered 1D grating we consider a structure with a modulation depth as a function of *z* such that the coupling parameter, κ, defined above, is a (not too large) constant. This choice is probably not the most efficient one for adiabatic excitation, but it enables analytical expressions for quantities like modulation depth distribution (see below), unlike more sophisticated structures (e.g., see (Povinelli *et al.* 2005)), resulting from more complicated procedures.

The above choice of constant κ is a reasonable one, as can be seen from Equation (16). Assuming that mode coupling is indeed small, such that $a(z) \approx a_0$ (i.e., is approximately constant), and that β variations and the term with κ_{bb} may be neglected, it follows from Equation (16), with $\kappa_{ba} \approx \kappa$:

$$b(z) \approx i a_0 \exp(i\beta z)\kappa z \,\mathrm{sinc}(\beta z). \tag{24}$$

From Equation (24) it can be seen that

$$|b(z)|^2 \lesssim |a_0 \kappa / \beta|^2, \tag{25}$$

so that no coherent build up of amplitude *b* will occur if κ is sufficiently small.

With the assumed constant κ it follows by integration from Equation (22)

$$n_m(z) \approx n_{m,edge} \tanh(\kappa z / C). \tag{26}$$

From the above the following relations can be derived:

$$L \approx C/\kappa \tanh^{-1}(n_{m,L} / n_{m,edge}), \tag{27}$$

and

$$\eta_L \approx \cosh(\kappa L / C) \approx \exp(\kappa L / C)/2, \tag{28}$$

where we also used Equation (23) and (for the second equality in Equation (28)) that in most cases of practical interest $\eta_L \gg 1$.

As an illustration to the above we have plotted in Fig. (7a) modulation depth profiles, the transmission, $T(\equiv |a(L)/a(0)|^2$ and the enhancement for a structure with a length of $L = 1mm$, a coupling constant such that the enhancement according to Equation (28) is $\eta_L = 100$ ($\kappa = 2.76/\mu m$) at wavelengths corresponding to $n_{m,edge} = 0.1,\ 0.2,\ 0.3$ ($\lambda = 0.9608,\ 0.9256,\ 0.8954 \mu m$). The numerical calculations presented in Fig. (7b) are on the basis of the transfer matrix method, starting at $z = L$ with $a(L) = 1$ and $b(L) = 0$.

For comparison also different taper profiles have been considered. In Fig. (8) the modal power is depicted for the profile given by Equation (26), a Gaussian profile $n_m(z) = n_{m,\max} \exp\{-[2(z-L)/L]^2\}$ and a linear profile $n_m(z) = n_{m,\max} z/L$. The results have been scaled such that the input power at the left is unity. In all cases the considered parameters are $\eta_L = 100$ and $L = 1mm$.

It can clearly be seen that the profile Equation (26) by far outperforms the others.

5. Discussion

In this section we will discuss the potential of tapered 1D gratings to obtain in practice large field enhancements, at low modal reflection. The effects of wavelength variation and fluctuations in structural are taken considered. Fig. (9) (left) shows the transmission curves as a function of the wavelength variation, $\delta\lambda$, for structures designed with the above procedure at wavelengths, λ_0, ($\delta\lambda = 0$), corresponding to $n_{m,edge} = 0.1$ and 0.3. The power enhancement, η_L, indicated in the graphs correspond to λ_0 ($n_{m,edge} = 0.1$ and 0.3). The sharp drop in transmission is due to the fact that at the corresponding wavelength the band edge is reached. The corresponding wavelength can be calculated to be (using $\delta\lambda = c_1(n_{m,edge} - n_{m,L})$): :

$$\delta\lambda \approx c_1 n_{m,edge}/(4\eta_L^2),\ c_1 = 0.35\mu m, \tag{29}$$

where we used Equation (23), rewritten as

$$\eta \approx \sqrt{n_{m,edge}/[2(n_{m,edge} - n_m)]}, \tag{30}$$

(using $n_m \approx n_{m,edge}$) and the approximate relation between wavelength and $n_{m,edge}$ ($\lambda = 1\mu m - c_1 n_{m,edge}$) following from a fit of the curve given in Fig. (5). From Equation (29) it can be seen that the demands on wavelength accuracy (and equivalently on thickness and index accuracy) are relatively high. E.g., for $\eta_L = 100$ it follows that $\delta\lambda/\lambda \approx 0.5\cdot 10^{-5}$. For smaller values of the enhancement a more practical value can be obtained, e.g. $\delta\lambda/\lambda \approx 0.5\cdot 10^{-3}$ if $\eta_L = 10$. Note that the requirements on wavelength accuracy relax somewhat for larger values of $n_{m,edge}$, according to Equation (29).

Equation 28 shows that for fixed wavelength in principle any value of η_L can be reached simply by increasing the product κL (and so, decreasing $n_{m,edge} - n_{m,L}$, see Equations (23) and (26)). However, the requirements on index accuracy increase (as on wavelength accuracy) proportional to $1/\eta_L^2$. From Equation (30) it can be seen that

$$\delta n \ll (n_{m,edge} - n_m) \approx n_{m,edge}/(4\eta_L^2), \tag{31}$$

where we made the seemingly reasonable assumption that the error in refractive indices, δn, should be smaller than the difference between applied modulation depth and that corresponding to the band edge. For unit cells with values of $\delta n > (n_{m,edge} - n_m)$ modal reflection will occur, as then the field solutions are evanescent corresponding to states within the band gap. Equation (31) leads to similar demands on the index accuracy as for $\delta\lambda/\lambda$. E.g. for $\eta_L = 10$ it follows from (31) that $\delta n \ll 10^{-3}$, assuming $n_{m,edge} \approx 0.4$. The above may hold for fabrication errors which extend over a longer range, including a large number of unit cells. A different requirement on index accuracy is obtained if a random fluctuation in modulation index, differing from unit cell to unit cell, is considered as discussed below.

As a final topic we consider random fluctuations, with a normal distribution with probability function $P(\delta n) = \exp(-\delta n^2/2)/\sqrt{2\pi}$, with a width of $|\delta n| \leq 10^{-3}$, of the

modulation depth in each unit cell. In order to obtain transmission (T) curves which are not too heavily fluctuating, all calculations presented in Fig. (10) are averaged over ten such calculations (implying a reduction in 'noise' by a factor of $\sim\sqrt{10}$). The length of the structure is 1mm, the coupling constant, κ, is such that the indicated value of η_L is attained at $\delta n = 0$, at wavelengths corresponding to $n_{m,edge} = 0.1$ and 0.3. From the graphs the following approximate relation can be obtained

$$|\delta n_{1/2}| \approx 4 \cdot 10^{-2} / \eta_L , \qquad (32)$$

where $\delta n_{1/2}$ indicates values corresponding to half of the maximum transmission. Note that the curves show only minor dependence on $n_{m,edge}$, and that $|\delta n_{1/2}| \propto 1/\eta_L$. If we assume a value of $|\delta n_{1/2}| \approx 10^{-3}$ is practically feasible it follows for the corresponding enhancement $\eta_L \approx 40$. Considering the 'noise' in the curves of Fig. (10) this means that a reasonable yield (of structures with not too large modal reflection, e.g. $T \gtrsim 0.5$) can be expected if devices aiming for values of $\eta_L \sim 40$ are fabricated under such practical conditions.

6. Conclusions

The paper presents results of calculations on 1D gratings with a varying modulation depth. Using a model structure approximate relation between power enhancement, the most relevant modal coupling parameter and structural parameters have been attained. A method for adiabatic tapering of 1D gratings was proposed, allowing for analytical expressions of among others the corresponding tapering profile. On the basis of the obtained expressions the practical feasibility of 1D gratings with large power enhancement, η, (and so with low group velocity) was discussed. It was found that, depending on the type of structural inaccuracies, a moderate enhancement of $\eta \sim 10-40$ seems possible, with not too low modal losses ($\lesssim 50\%$) at relative errors in the refractive indices, and also in the wavelength, of $\sim 10^{-3}$. The requirements on structural inaccuracies may relax somewhat in structures with larger index contrast than the assumed values (~0.3).

Acknowledgments

The authors thank T.P. Valkering for helpful discussions. Part of the project was funded by the Royal Netherlands Academy of Arts and Sciences (KNAW, project 99.WI.44).

References

Haus, H.A. *Waves and fields in optoelectronics*. Prentice-Hall Inc,. Englewood Cliffs, New Jersey, 1982.

Johnson, S., P. Bienstman, M. Sakrobogatiy, M. Ibanescu, E. Lidorikis, and J. Joannopoulos. *Phys. Rev. E* **66** 1, 2002.
Kogelnik, H. and C.V. Shank. *J. Appl. Phys.* **43** 2327, 1971.
Yablonovitch, E. *Phys. Rev. Lett.* **50** 2059, 1987.
Matuschek, N., F.X. Kärtner, and U. Keller. *IEEE J. Quantum Electron.* **33** 295, 1997.
Mekis, A. J. Chen, I. Kurland, S. Fan, P. Villeneuve, and J. Joannopoulos. *Phys. Rev. Lett.* **77** 3787, 1996.
Notomi, M., K. Yamada, A. Shinya, J. Takahashi, C. Takahashi, and I. Yokohoma. *Phys. Rev. Lett.* **87** 253902-1, 2001.
Povinelli, M.L., S.G Johnson, J.D. Joannopoulos. *Opt. Express* **13** 7145, 2005.
Sakoda, K. and K. Ohtaka, *Phys. Rev. B* **54** 5732, 1996.
Sipe, J.E., L. Poladian, and C. M. de Sterke. *J. Opt. Soc. Am. A.* **11** 1307, 1994.
Spielmann, Ch., R. Szipöcs, A. Stingl, and F. Krausz. *Phys. Rev. Lett.* **73** 2308, 1994.

Captions:

Fig. 1. Refractive index distribution as a function of *z* for a 1D tapered grating.
Fig. 2. Symmetric unit cell of a1D uniform grating. The arrows indicate incoming and outgoing plane waves.
Fig. 3. Transition between two unit cells with a different modulation depth. The arrows indicate incoming and outgoing modes.
Fig. 4. Relation between wavelength λ defining the band edge and the corresponding modulation depth, $n_{m,edge}$.
Fig. 5. Numerically calculated curves (dashed) and curves according to Equations (22) and (23) (solid) of the quantities $\Omega_1 \equiv \kappa h / \partial_z n_m$ (a) and $\Omega_2 = \eta\sqrt{h}$ (b) as a function of n_m and $n_{m,edge}$.
Fig. 6. Dispersion curves for the considered model structure for $n_m = 0$ (dotted curve) and 0.01, 0.05, 0.1 and 0.3. The dashed arrow indicates the trajectory for adiabatic excitation.
Fig. 7. (a) Index profile $n_m(z)$ and $\log_{10}(\Lambda\partial_z n_m)$ as a function of *z*. (b) The corresponding power enhancement, η_L, according to Equation (28) (squares) and obtained with the transfer matrix method (solid line). The transmission, *T*, according to the latter is also given. Note that the quantity $\Lambda\partial_z n_m$ is the change in modulation depth per unit cell.
Fig. 8. Dependence on *z* of modal power for structures with the indicated type of tapering (see text). The wavelength corresponds to $n_{m,edge} = 0.3$.
Fig. 9. Calculated dependence on small wavelength variations of transmission, *T*, and enhancement η_L for adiabatic structures designed to have the indicated enhancement at wavelengths λ_0 ($\delta\lambda = 0$). At the right hand side of the right figures η_L blows up (not shown here).

Fig. 10. Relation between modal transmission, *T*, and random variations with a normal distribution (half width δn) in the modulation depth for two different wavelengths (corresponding to $n_{m,edge} = 0.1$ and 0.3).

Figures

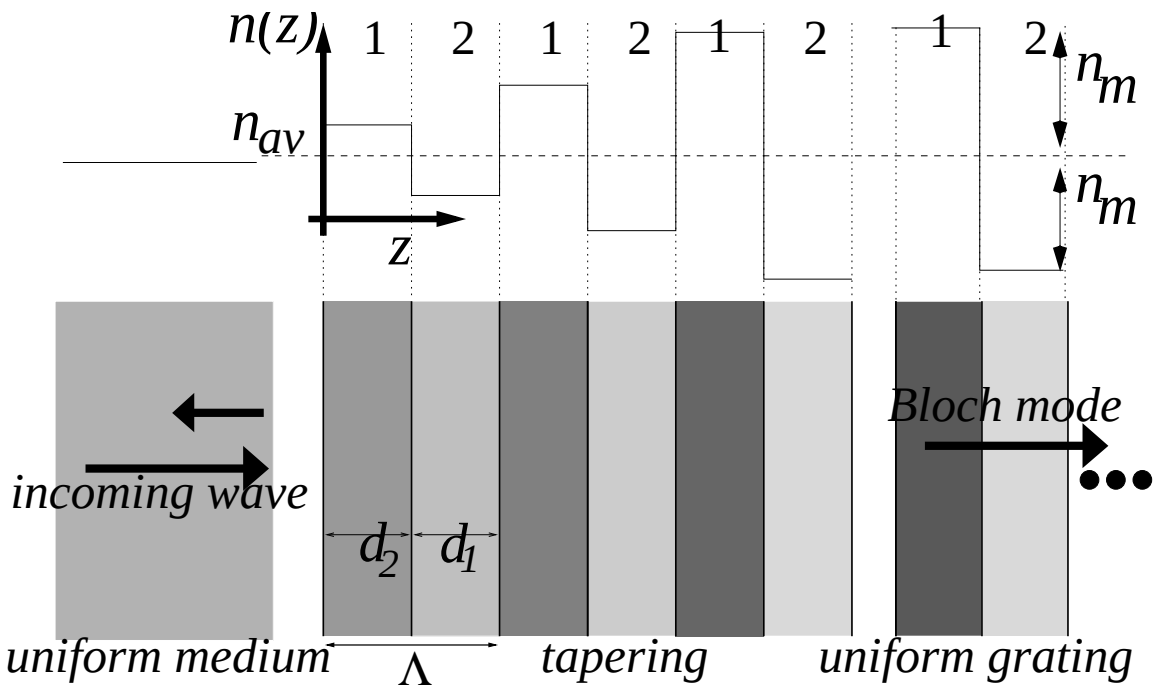

Figure 1

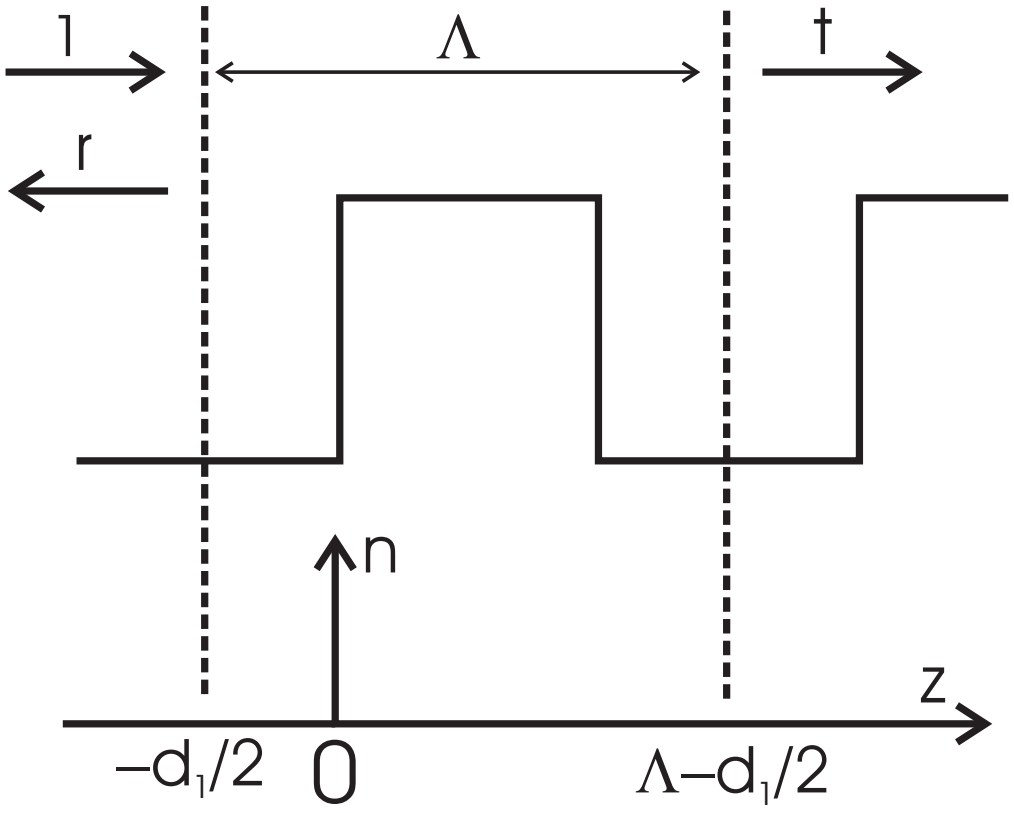

Figure 2

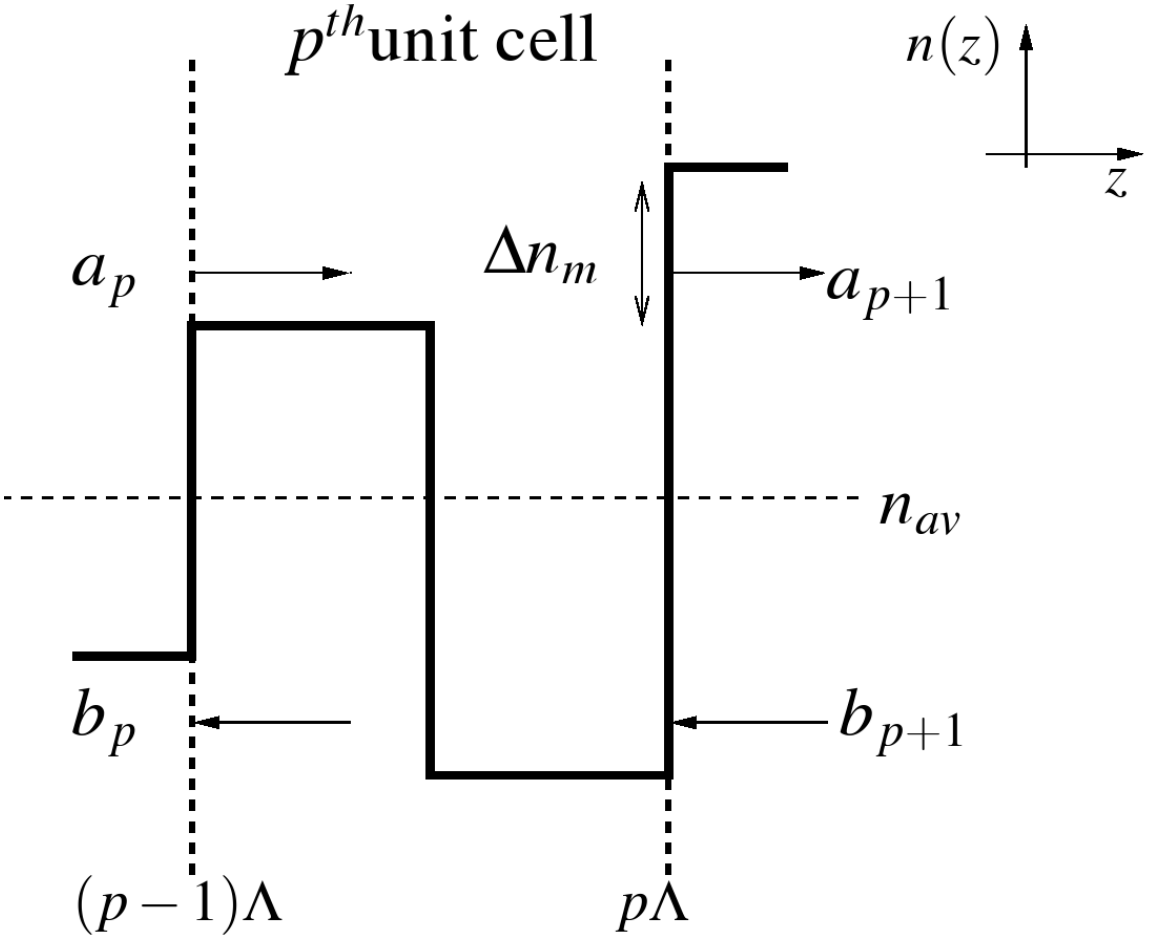

Figure 3

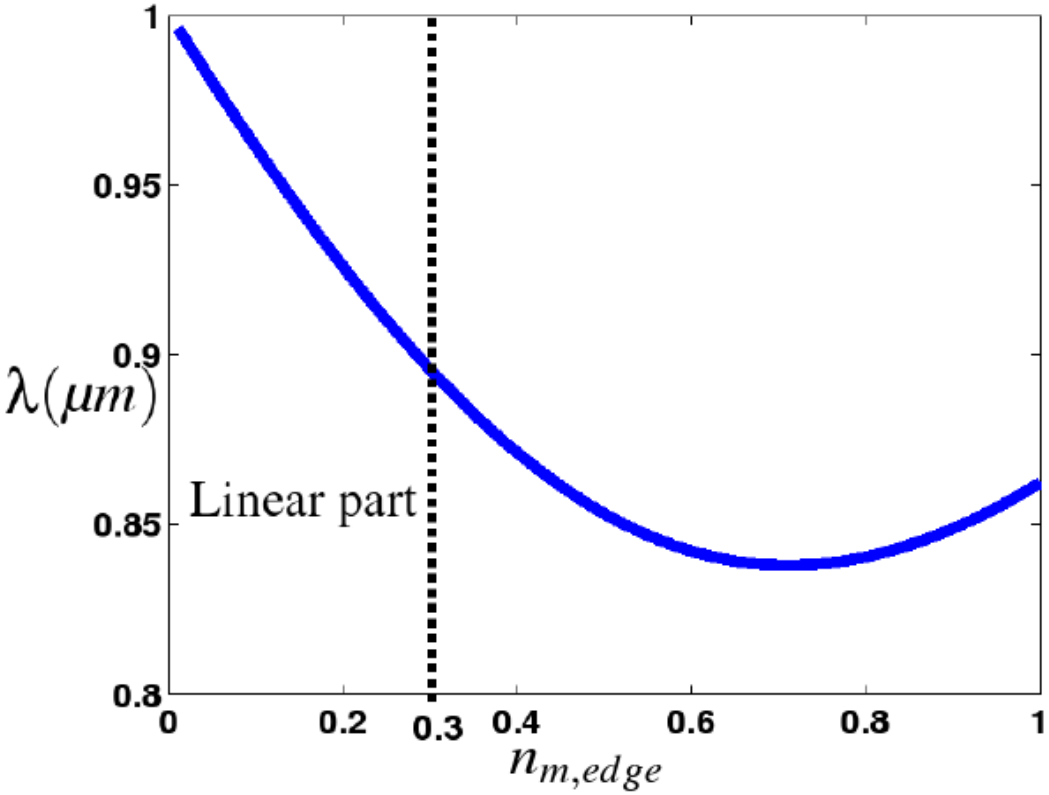

Figure 4

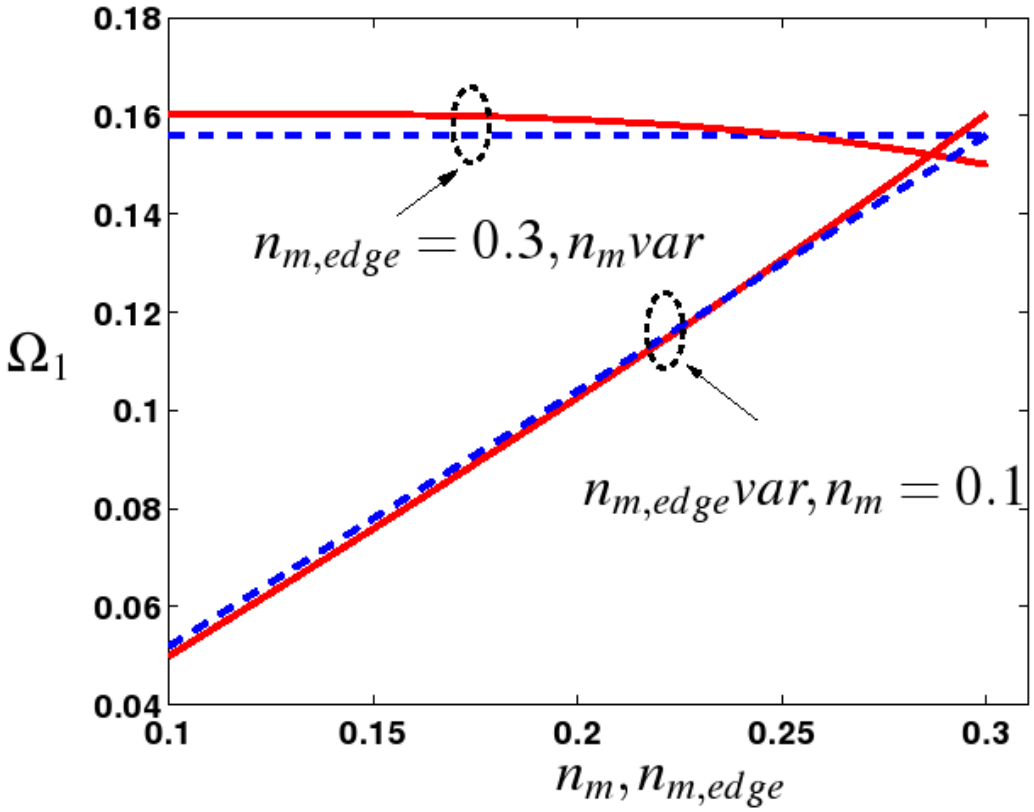
0.18
0.16
0.14
0.12
0.1
0.08
0.06
0.04
0.1
0.15
0.2
0.25
0.3
Ω_1
$n_m, n_{m,edge}$
$n_{m,edge} = 0.3, n_m var$
$n_{m,edge} var, n_m = 0.1$

Figure 5a

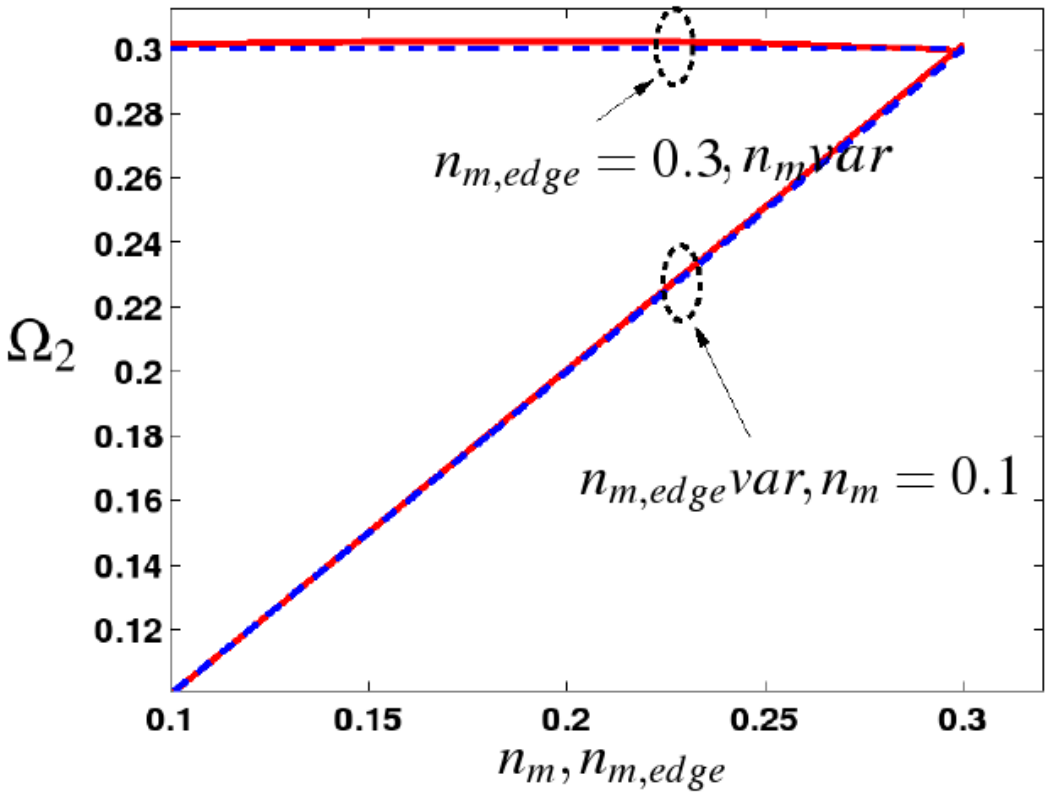
0.3
0.28
0.26
0.24
0.22
0.2
0.18
0.16
0.14
0.12
Ω_2
$n_{m,edge} = 0.3, n_m var$
$n_{m,edge} var, n_m = 0.1$
0.1
0.15
0.2
0.25
0.3
$n_m, n_{m,edge}$

Figure 5b

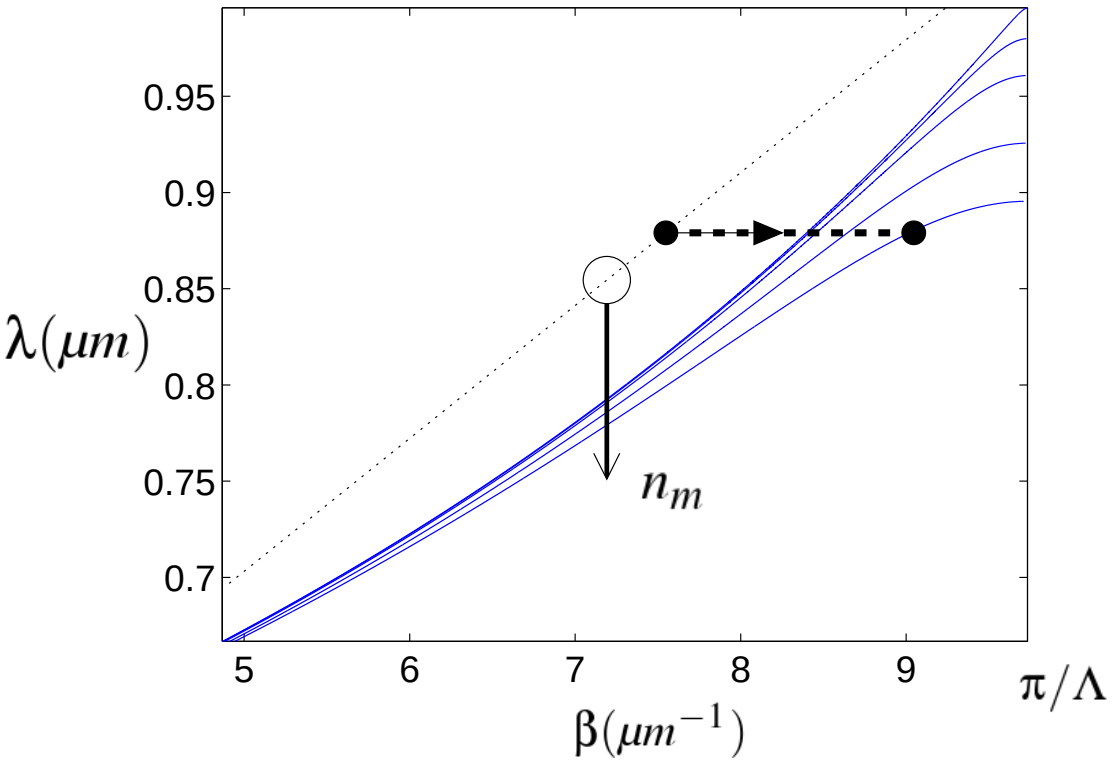

Figure 6

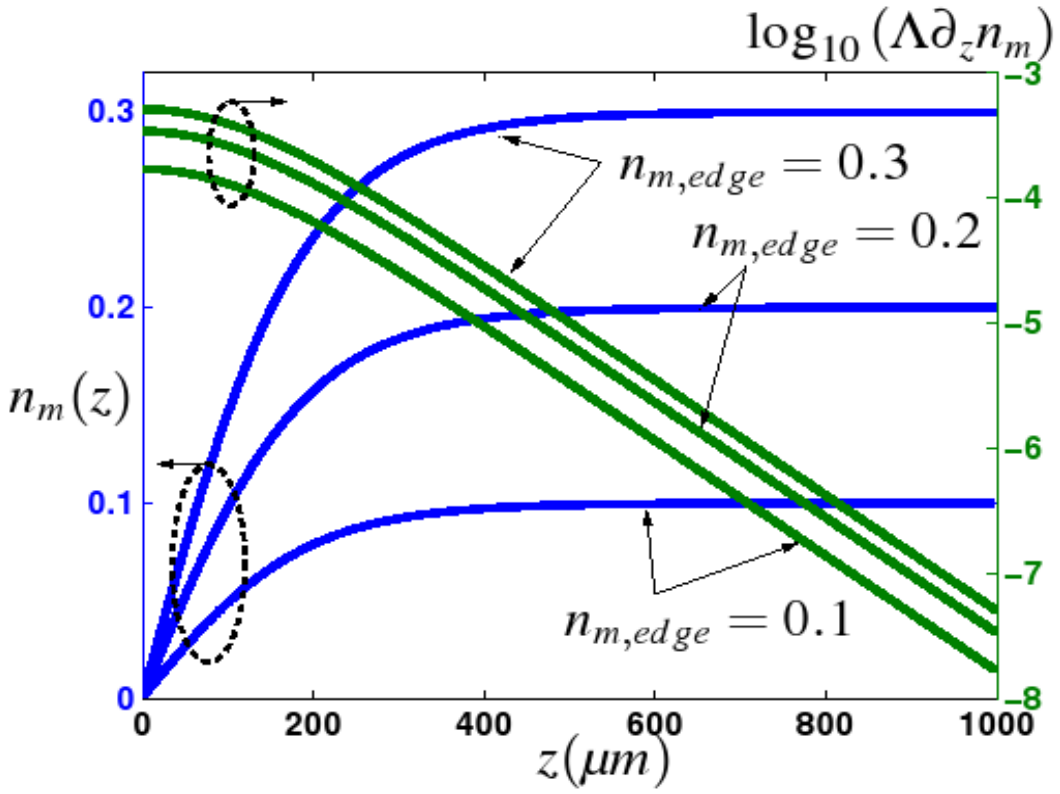
$\log_{10}(\Lambda\partial_z n_m)$
$n_m(z)$
$z(\mu m)$
$n_{m,edge} = 0.3$
$n_{m,edge} = 0.2$
$n_{m,edge} = 0.1$
0
0.1
0.2
0.3
0
200
400
600
800
1000
−3
−4
−5
−6
−7
−8

Figure 7a

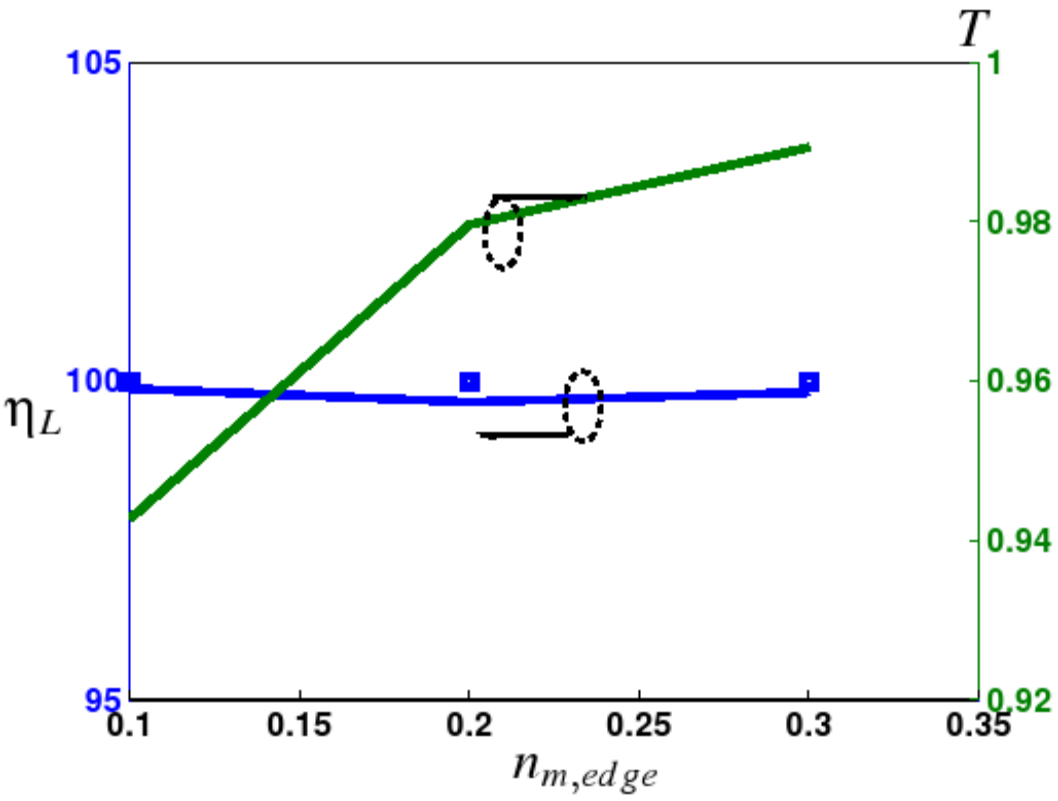

Figure 7b

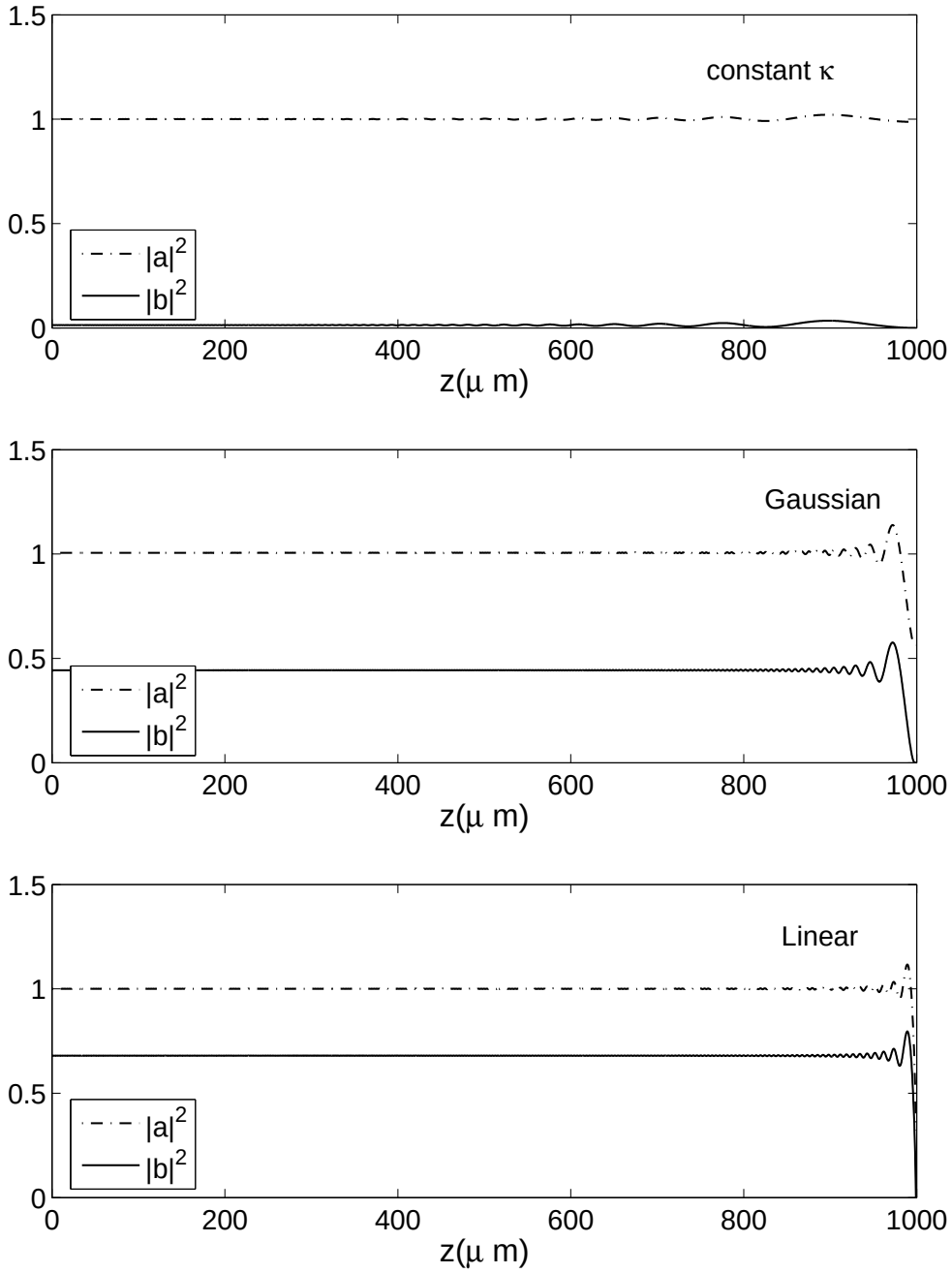
constant κ
|a|2
|b|2
z(μ m)
Gaussian
|a|2
|b|2
z(μ m)
Linear
|a|2
|b|2
z(μ m)
0
0.5
1
1.5
200
400
600
800
1000

Figure 8

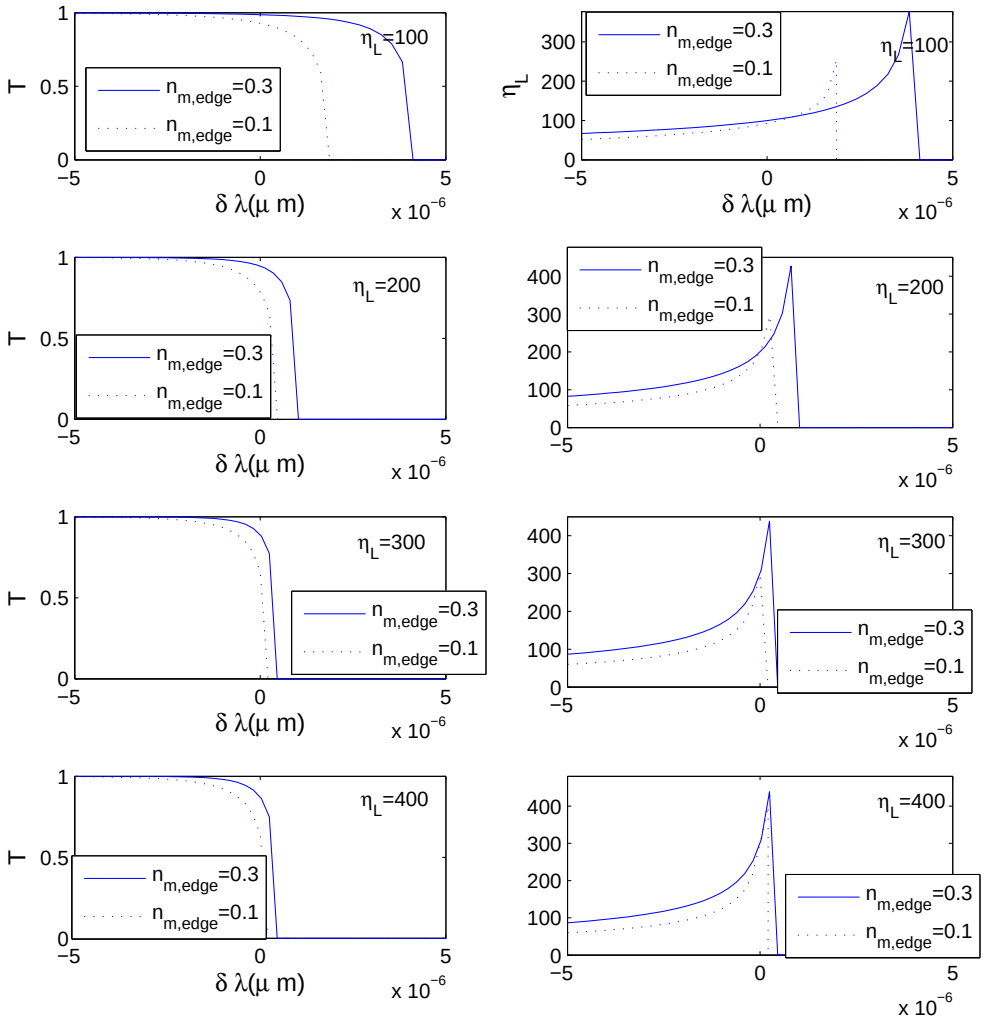

Figure 9

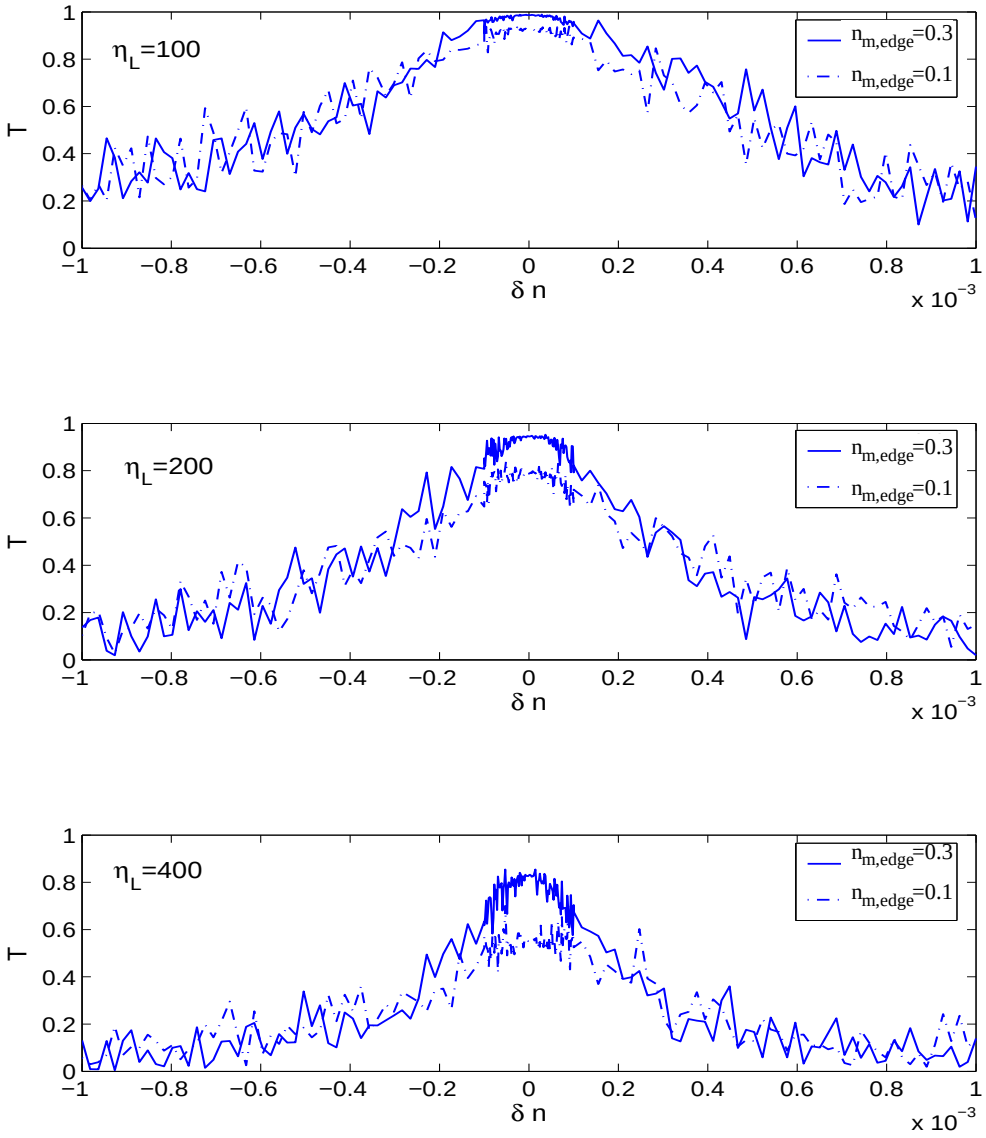
η_L=100
n_m,edge=0.3
n_m,edge=0.1
T
δ n
x 10^-3
η_L=200
n_m,edge=0.3
n_m,edge=0.1
T
δ n
x 10^-3
η_L=400
n_m,edge=0.3
n_m,edge=0.1
T
δ n
x 10^-3

Figure 10